

## Computational Methods for High-Resolution Gravity Field Modeling

Róbert Čunderlík, Karol Mikula, Zuzana Minarechová and Marek Macák

Department of Mathematics and Descriptive Geometry, Faculty of Civil Engineering, Slovak University of Technology, Bratislava, Slovakia

### Definition

Computational methods, like the boundary element, finite element, or finite volume methods, are numerical discretization methods that can be used for high-resolution gravity field modeling. They are efficient to solve the geodetic boundary value problems in a space domain. To obtain high-resolution numerical solutions usually lead to large-scale parallel computations that can be performed using high-performance computing (HPC) facilities.

### Introduction

A determination of the Earth's gravity field is usually formulated in terms of the geodetic boundary value problems (BVPs). There exist various numerical approaches to solve such potential problems. In geodesy, the spherical harmonics (SH) based methods are usually used for global gravity field modeling. They solve the problem in a frequency domain, and nowadays, they have become a very efficient and sophisticated tool. A recent development of high-performance computing (HPC) facilities has brought new opportunities for numerical solutions of the geodetic BVPs. Efficient numerical methods, such as the boundary element method (BEM), finite element method (FEM), or finite volume method (FVM), can be also applied for global or local gravity field modeling. These discretization methods solve geodetic BVPs (GBVPs)

in a space domain. In order to obtain precise numerical solutions, they usually require very refined discretizations leading to large-scale computations. On the other hand, parallel implementations of algorithms and high-performance computations on clusters with distributed memory provide strong opportunities for high-resolution gravity field modeling. In this chapter, there are mentioned recent efficient parallel computational approaches for solving GBVPs.

### Fixed Gravimetric Boundary Value Problem

To present the computational methods, we outline numerical solutions to the linearized fixed gravimetric boundary value problem (FGBVP) (Koch and Pope 1972; Holota 1997; Čunderlík et al. 2008; Fašková et al. 2010; Minarechová et al. 2015):

$$\Delta T(\mathbf{x}) = 0, \mathbf{x} \in R^3 - S, \quad (1)$$

$$\langle \nabla T(\mathbf{x}), \vec{s}(\mathbf{x}) \rangle = -\delta g(\mathbf{x}), \quad \mathbf{x} \in \partial S, \quad (2)$$

$$T(\mathbf{x}) \rightarrow 0, \quad \text{as } |\mathbf{x}| \rightarrow \infty, \quad (3)$$

where  $\Delta$  is the Laplace operator,  $T(\mathbf{x})$  is the disturbing potential defined as the difference between the real  $W(\mathbf{x})$  and the normal  $U(\mathbf{x})$  gravity potential at any point  $\mathbf{x}$ ,  $S$  denotes the Earth body,  $\langle, \rangle$  represents the inner product of vectors,  $\nabla$  is the gradient operator,  $\vec{s}(\mathbf{x}) = -U(\mathbf{x}) / |U(\mathbf{x})|$  is the unit vector normal to the equipotential surface of the normal potential  $U$  at point  $\mathbf{x}$ , and  $\delta g(\mathbf{x})$  is the so-called gravity disturbance.

Equations (1)–(3) represent an exterior BVP for the Laplace equation, i.e., the computational domain (outside the Earth) is infinite. From the aforementioned numerical methods, it is natural to apply BEM that is suitable for exterior BVPs since it reduces the problem from the 3D infinite domain onto its “2D” boundary. On the contrary, FEM and

FVM require a discretization of the whole computational domain into finite 3D elements or volumes. Although there exists a possibility to use infinite elements (Šprlák et al. 2011), in standard approaches one has to consider a bounded computational domain. To that goal we construct a domain  $\Omega$  in the external space above the Earth (see Fašková et al. 2010). The domain  $\Omega$  is bounded by the bottom surface  $\Gamma \subset \partial\Omega$  representing the Earth's surface and the upper surface at the level of chosen satellite mission, where the Dirichlet-type boundary conditions (BC) for disturbing potential are generated from some satellite-only geopotential model.

In the bounded domain  $\Omega$ , we consider the FGBVP in the following form:

$$\Delta T(\mathbf{x}) = 0, \quad \mathbf{x} \in \Omega, \quad (4)$$

$$\langle \nabla T(\mathbf{x}), \vec{s}(\mathbf{x}) \rangle = -\delta g(\mathbf{x}), \quad \mathbf{x} \in \Gamma, \quad (5)$$

$$T(\mathbf{x}) = T_{\text{SAT}}(\mathbf{x}), \quad \mathbf{x} \in \partial\Omega - \Gamma \quad (6)$$

where  $T_{\text{SAT}}$  represents the disturbing potential generated from the satellite-only geopotential model. Since in this case we deal with the solution in the bounded domain  $\Omega$ , we do not prescribe any regularity condition at infinity.

The boundary condition given by Eq. (2) or (5) represents the oblique derivative BC since the vector  $\vec{s}$  does not coincide with the normal to the Earth's surface. For simplicity, in the following sections we will consider them as the Neumann BC. It is due to the fact that in all presented numerical experiments we use ellipsoidal approximation of the Earth's surface. Hence, the problem of oblique derivatives vanishes because  $\vec{s} = \vec{n}_\Gamma$ , where  $\vec{n}_\Gamma$  is the normal to the computational domain  $\Omega$ .

## Boundary Element Method

An objective of the boundary element method is to replace a partial differential equation (PDE) solved in a 3D domain by an equivalent equation that gives a solution on the domain boundary only (c.f. Brebbia et al. 1984; Hartmann 1989; Schatz et al. 1990; Lucquin and Pironneau 1998). There are two fundamental approaches to derive an integral formulation of the Laplace equation on the domain boundary. The first one is often called the direct method and the integral equations can be derived through an application of the Green's third identity. The second technique is called the indirect method, which is based on the assumption that harmonic functions can be expressed in terms of a single-layer or double-layer potential generated by continuous source density functions defined on the boundary.

A main advantage of BEM arises from the fact that only the boundary of the solution domain requires a subdivision into its elements. Thus the dimension of the problem is effectively reduced by one. The direct BEM formulation

applied to the linearized FGBVP in Eqs. (1)–(3) results in the boundary integral equation (BIE)

$$\frac{1}{2}T(\mathbf{x}) + \int_\Gamma T(\mathbf{y}) \frac{\partial G(\mathbf{x}, \mathbf{y})}{\partial n_\Gamma(\mathbf{y})} d\mathbf{y} = \int_\Gamma \frac{\partial T}{\partial n_\Gamma}(\mathbf{y}) G(\mathbf{x}, \mathbf{y}) d\mathbf{y}, \quad (7)$$

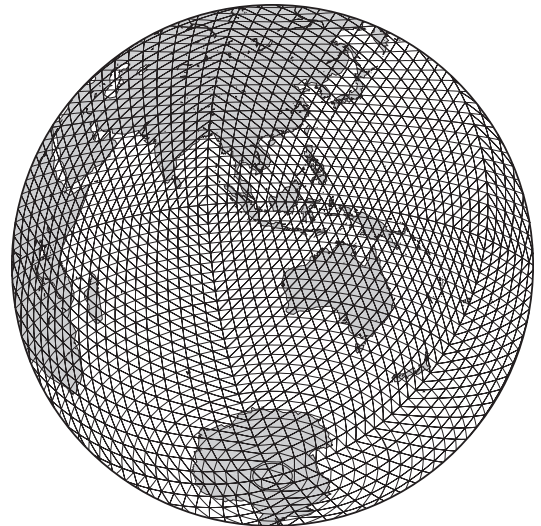
$\mathbf{x} \in \Gamma$ , where  $n_\Gamma$  is the normal to the boundary  $\Gamma$  (the Earth's surface) and the kernel function  $G$  represents the fundamental solution of the Laplace equation,

$$G(\mathbf{x}, \mathbf{y}) = \frac{1}{4\pi |\mathbf{x} - \mathbf{y}|}, \quad \mathbf{x}, \mathbf{y} \in R^3. \quad (8)$$

Neglecting the problem of the oblique derivative, input gravity disturbances in Eq. (2) directly represent  $\frac{\partial T}{\partial n_\Gamma}$  in BIE (7). The collocation method with linear basis functions (denoting by  $C^1$  collocation) can be used to derive the linear system of equations from BIE (7). The Earth's surface (or its ellipsoidal approximation) is approximated by a triangulation of the topography expressed as a set of panels  $\Delta T_j$  (Fig. 1). The vertices  $\mathbf{x}_i$  of the triangles represent the collocation points. The  $C^1$  collocation involves approximation of the boundary functions by a linear function on each triangle (Brebbia et al. 1984),

$$T(\mathbf{x}) \approx \sum_{k=1}^3 T_k \Psi_k(\mathbf{x}), \quad \mathbf{x} \in \Delta\Gamma_j, \quad (9)$$

$$\delta g(\mathbf{x}) \approx \sum_{k=1}^3 \delta g_k \Psi_k(\mathbf{x}), \quad \mathbf{x} \in \Delta\Gamma_j, \quad (10)$$



**Computational Methods for High-Resolution Gravity Field Modeling, Fig. 1** Discretization of the Earth's surface by the global triangulation

where  $T_k$  and  $\delta g_k$  for  $k = 1, 2, 3$  represent values of the boundary functions at the vertices of the triangle  $\Delta\Gamma_j$ . The linear basis functions  $\Psi_1, \Psi_2, \dots, \Psi_N$  are given by

$$\Psi_j(\mathbf{x}_i) = 1, \quad \mathbf{x}_i = \mathbf{x}_j, \quad (11)$$

$$\Psi_j(\mathbf{x}_i) = 0, \quad \mathbf{x}_i \neq \mathbf{x}_j, \quad (12)$$

where  $i = 1, \dots, N; j = 1, \dots, N$  and  $N$  is the number of the collocation points. These approximations allow to reduce BIE (7) to a discrete form (Čunderlík et al. 2008)

$$\begin{aligned} c_i T_i \Psi_i + \sum_{j=1}^N \int_{\text{supp}\Psi_j} \frac{\partial G_{ij}}{\partial n_\Gamma} T_j \Psi_j d\Gamma_j &= \\ &= \sum_{j=1}^N \int_{\text{supp}\Psi_j} G_{ij} \delta g_j \Psi_j d\Gamma_j, \quad i = 1, \dots, N, \end{aligned} \quad (13)$$

where  $\text{supp}\Psi_j$  is the support of the  $j$ th basis function. The coefficient  $c_i$  represents a ‘‘spatial segment’’ bounded by the triangles joined at the  $i$ th collocation point. In the case of the linear basis functions, it can be evaluated by the expression (Mantič 1993)

$$c_i = \frac{1}{4\pi} \left[ 2\pi + \sum_{s=1}^S \text{sgn}(r^i \cdot \langle n^s, n^{s+1} \rangle) \text{arc cos}(n^s \cdot n^{s+2}) \right], \quad (14)$$

where  $r^i$  is the distance vector at the  $i$ th collocation point,  $n^s$  is the normal unit vector to the  $s$ th triangle of the  $\text{supp}\Psi_i$ , and  $S$  represents the number of triangles in the  $\text{supp}\Psi_i$ . In fact, Eq. (13) represent the system of linear equations that can be rewritten into the matrix-vector form

$$\mathbf{M}\mathbf{t} = \mathbf{L}\delta\mathbf{g}, \quad (15)$$

where  $\mathbf{t} = (T_1, \dots, T_N)^T$  and  $\delta\mathbf{g} = (\delta g_1, \dots, \delta g_N)^T$ . Coefficients of the matrices  $\mathbf{M}$  and  $\mathbf{L}$  represent integrals that need to be computed using an appropriate discretization of the integral operators in (13). The discretization of the integral operators is affected by the weak singularity of the kernel functions. The integrals with regular integrands, which represent nondiagonal coefficients, are approximated by the Gaussian quadrature rules defined on a triangle (Laursen and Gellert 1978). Their discrete form is given by

$$L_{ij} = \frac{1}{4\pi} \sum_{s=1}^S A_{j_s} \sum_{k=1}^K \frac{1}{r_{ik_s}} \Psi_k w_k, \quad i \neq j \quad (16)$$

$$M_{ij} = \frac{1}{4\pi} \sum_{s=1}^S A_{j_s} k_{ij_s} \sum_{k=1}^K \frac{1}{r_{ik_s}^3} \Psi_k w_k, \quad i \neq j \quad (17)$$

where  $A_{j_s}$  is the area of the  $s$ th triangular element of the  $\text{supp}\Psi_j$ ,  $k_{ij_s}$  is the distance from the  $i$ th collocation point to the plane represented by this triangular element,  $K$  is the number of points used for the Gaussian quadrature with their corresponding weights  $w_k$  and linear basis functions  $\Psi_k$ , and  $r_{ik_s}$  is the distance from the  $i$ th collocation point to the  $k$ th quadrature point of the  $s$ th triangular element. The  $j$ th component of the vector  $\delta\mathbf{g}$  in (15) corresponds to the input value of the measured surface gravity disturbance  $\delta g$  at the  $j$ th collocation point. The nonregular integrals (singular elements) arise only for the diagonal components of the linear system. They require special evaluation techniques in order to handle the singularity of the kernel function. Thanks to the diagonal component  $c_i$  and the orthogonality of the normal to its planar triangular element, the singular element is represented by the spatial segment (Baláš et al. 1989)

$$M_{ii} = c_i. \quad (18)$$

The kernel function  $G$  (Eq. (8)) in integrals on the right-hand side of Eq. (13) is weakly singular. Hence, the diagonal coefficients  $L_{ii}$  can be evaluated analytically

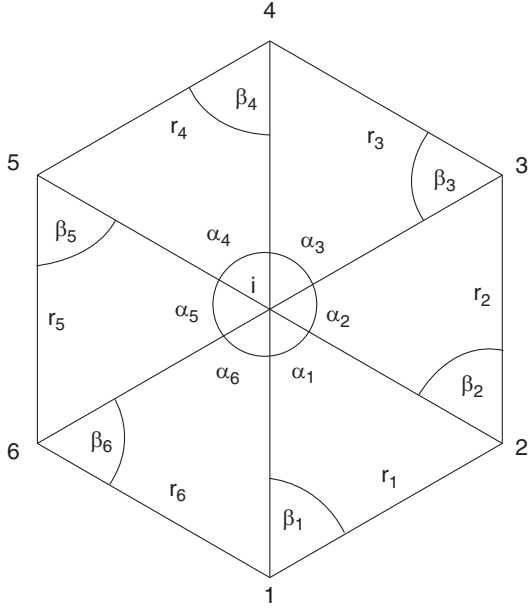
$$L_{ii} = \frac{1}{2\pi} \sum_{s=1}^S \frac{A_{i_s}}{r_s} \ln \frac{\text{tg}[(\beta_s + \alpha_s)/2]}{\text{tg}(\beta_s/2)}. \quad (19)$$

where  $A_{i_s}$  is the area of the  $s$ th triangle of the  $\text{supp}\Psi_i$  determined by the line of length  $r_s$  and angles  $\alpha_s, \beta_s$  (Fig. 2).

The diagonal component in Eq. (18) can be evaluated geometrically using (14) or through the physical consideration. The second approach is based on the fact that a constant potential applied over a closed body produces no flux. Accordingly, in case of the exterior Neumann problems, the sum of all components in each row should be equal to 1 (Brebbia et al. 1984). Then one can easily calculate the coefficient  $M_{ii}$  after evaluating of all nondiagonal coefficients of the matrix  $\mathbf{M}$  using the Gaussian quadrature in Eq. (17)

$$M_{ii} = 1 - \sum_{j=1, i \neq j}^N M_{ij}. \quad (20)$$

The matrix  $\mathbf{M}$  in Eq. (15) is a nonsymmetric dense  $N \times N$  matrix. However, the decay of the kernel function  $\partial G/\partial n_\Gamma$  makes the stiffness matrix generally well conditioned. Consequently, nonstationary iterative methods can be applied to solve this large-scale linear system of equations. The Bi-Conjugate Gradient Stabilized (BiCGSTAB) method



**Computational Methods for High-Resolution Gravity Field Modeling, Fig. 2** Evaluating of the singular element (the  $C^1$  collocation)

(Barrett et al. 1994), which is suitable for dense and non-symmetric matrices, can be used efficiently.

## Finite Element Method

In the contrary to BEM, where the domain dimension is reduced by one, in the finite element method we discretize the original computational domain. To obtain a discrete form of the Laplace equation in the domain  $\Omega$ , the Green theorem is applied. First, we multiply the differential equation (4) by a function  $v \in V$ , where  $V$  is the so-called Sobolev space (Rektorys 1974; Brenner and Scott 2002; Fašková et al. 2010) and we use the Green theorem to obtain an identity

$$\int_{\Omega} \nabla T \cdot \nabla v \, d\mathbf{x} - \int_{\partial\Omega} \nabla T \cdot \mathbf{n}_{\partial\Omega} v \, d\sigma = 0, \quad \forall v \in V. \quad (21)$$

If the extension of the Dirichlet BC given by  $T_{SAT}$  into the domain  $\Omega$  be in  $W_2^{(1)}(\Omega)$  and  $\delta g \in L^2(\Gamma)$ , we can define the so-called weak formulation of the FGBVP (4)–(6) as follows: we look for a function  $T$ , such that  $T - T_{SAT} \in V$  and the identity

$$\int_{\Omega} \nabla T \cdot \nabla v \, d\mathbf{x} + \int_{\Gamma} \delta g v \, d\sigma = 0, \quad (22)$$

holds for  $\forall v \in V$ . According to Rektorys (1974) and Brenner and Scott (2002), the solution of this weak formulation always exists and is unique. Moreover, the finite element approximation converges to the weak solution  $T$  refining the finite element grid.

The FEM assumes a discretization of the domain  $\Omega$  into finite elements. Let  $V_h$  be a finite dimensional subspace of  $V$ , corresponding to the finite element grid with a basis given by (11) and (12), where  $x_i$  are now nodes of 3D tetrahedral elements.

If we write  $T^n(\mathbf{x}) = \sum_{j=1}^n t_j \Psi_j(\mathbf{x})$ , namely we take an approximation of  $T$  as  $T^n$ , i.e., a linear combination of basis functions with coefficients  $t_i$ ,  $i = 1, \dots, n$ , where  $n$  is the number of grid nodes, plug it into Eq. (22) and consider  $v = \Psi_i$ , we obtain

$$\sum_{j=1}^n t_j \phi(\Psi_i, \Psi_j) = q_i \quad i = 1, \dots, n, \quad (23)$$

where  $\phi(\Psi_i, \Psi_j) = \int_{\Omega} \Psi_i \cdot \Psi_j \, d\mathbf{x}$ ,  $q_i = - \int_{\Gamma} \delta g \Psi_i \, d\sigma$ .

Let the column vectors  $(t_1, \dots, t_n)$ ,  $(q_1, \dots, q_n)$  be denoted by  $\mathbf{t}$  and  $\mathbf{q}$ , and let  $\mathbf{K} = [K_{ij}]_{n \times n}$  be the matrix with entries  $K_{ij} = \phi(\Psi_i, \Psi_j)$ . Then Eq. (23) can be written as

$$\mathbf{K}\mathbf{t} = \mathbf{q}, \quad (24)$$

which represents the linear system of equations for unknown nodal solution values  $\mathbf{t}$ . The matrix  $\mathbf{K}$  is a sparse, symmetric, and positive definite matrix, and the system can be solved by a suitable standard solver. The more details about FEM approach can be found in Fašková et al. (2010).

## Finite Volume Method

Similarly to FEM, also in the finite volume method, the computational domain is divided into a number of finite volumes denoted by  $p$ . We multiply the Laplace equation (4) by minus one and integrate it over a finite volume  $p$ . Using the divergence theorem

$$- \int_p \Delta T \, d\mathbf{x} = - \int_{\partial p} \langle \nabla T, \vec{n} \rangle \, d\mathbf{x}, \quad (25)$$

we obtain for every finite volume  $p$  the equation

$$-\int_{\partial p} \frac{\partial T}{\partial n} d\mathbf{x} = 0. \quad (26)$$

Let  $q \in N_p$  be a neighbor of finite volume  $p$ , where we have denoted by  $N_p$  all neighbors which have common side with  $p$ . Then let  $T_p$  and  $T_q$  be the approximate values of  $T$  in  $p$  and  $q$ ,  $e_{pq}$  is a boundary of the finite volume  $p$  common with  $q$ ,  $\vec{n}_{pq}$  is its unit normal vector oriented from  $p$  to  $q$ , and  $m(e_{pq})$  is the area of  $e_{pq}$ . Let  $\mathbf{x}_p$  and  $\mathbf{x}_q$  be representative points of  $p$  and  $q$  (e.g., centers of gravity) and  $d_{pq}$  their Euclidean distance. Let us approximate the normal derivative along the boundary of the volume  $p$  by

$$\frac{\partial T}{\partial n_{pq}} \approx \frac{T_q - T_p}{d_{pq}}. \quad (27)$$

Then from (26) and (27) we obtain for every finite volume  $p$  an equation

$$-\sum_{q \in N_p} \frac{T_q - T_p}{d_{pq}} m(e_{pq}) = 0. \quad (28)$$

Finally, after rearrangement we have

$$\sum_{q \in N_p} \frac{m(e_{pq})}{d_{pq}} (T_p - T_q) = 0, \quad (29)$$

which represents the linear system of algebraic equations for the FVM approximation of the Laplace equation (4). The term  $\frac{m(e_{pq})}{d_{pq}}$  defined for the finite volume  $p$  and its neighbor  $q$  is referred to as the transmissivity coefficient (see, e.g., Eymard et al. 2001). The system of coefficients and the right-hand side vector are modified for finite volumes along the boundary of the computational domain. For the finite volumes along side and upper boundaries (case of the Dirichlet BCs), we prescribe the disturbing potential  $T_{\text{SAT}}$  for  $T_q$  in (29), and move the term  $-\frac{m(e_{pq})}{d_{pq}} T_q$  to the right-hand side. For the Neumann-type BCs applied on the bottom boundary, we prescribe for  $\delta g$  the value  $\frac{T_q - T_p}{d_{pq}}$  in (29), see also (27), and move  $m(e_{pq}) \delta g$  to the right-hand side and update the diagonal coefficient. Using

these approaches, we get the right-hand side vector with nonzero entries and modified diagonal coefficients for finite volumes along the boundary. The matrix of the system is nonsymmetric and diagonal dominant, so the iterative solvers as BiCGSTAB can be used efficiently. The more details about FVM approach can be found in Minarechová et al. (2015)).

## Numerical Experiments

To demonstrate properties of the presented numerical approaches, a reconstruction of a known harmonic function using BEM, FEM, or FVM is presented. The harmonic function has been generated by the SH approach, namely the disturbing potential has been evaluated from the EGM2008 geopotential model up to degree and order 2160 (Pavlis et al. 2012). In all experiments of global modeling, an ellipsoidal approximation of the Earth's surface has been considered. The Neumann BC evaluated from the EGM2008 coefficients have been prescribed in the form of the first derivatives of the disturbing potential in the direction of the normal to the ellipsoid.

In case of BEM, the ellipsoidal surface has been approximated by the global triangulation (Fig. 1). Table 1 summarizes statistical characteristics of the residuals between the BEM solutions and EGM2008 for different levels of the discretization. Figure 4a depicts the residuals for the finest discretization, i.e., the size of triangles is about 3 arc min and 12960002 nodes (collocation points) are uniformly distributed over the ellipsoid. To achieve such a high-resolution modeling, a parallelization of algorithms using the MPI (Message Passing Interface) subroutines has been implemented. Moreover, an elimination of far zones' contributions was practically inevitable and the iterative procedure introduced in (Čunderlík and Mikula 2010) has been used.

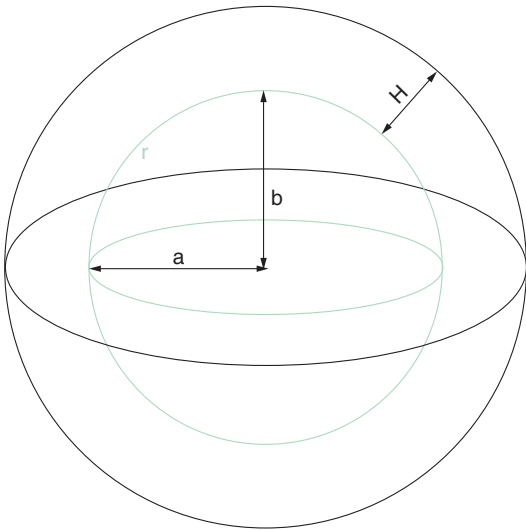
In case of FEM or FVM, the 3D computational domain (Fig. 3) between the ellipsoid and upper boundary located at the constant altitude 240 km above the ellipsoid has to be discretized. Consequently, the number of nodes is much higher than in case of BEM. On the other hand, the system matrices in Eq. (24) or (29) are sparse, therefore they lead to smaller memory requirements. However, to achieve high-resolution modeling, parallel implementations are necessary as well. In case of FEM, the parallel version of the ANSYS

**Computational Methods for High-Resolution Gravity Field Modeling, Table 1** Statistical characteristics of the residuals between the BEM solutions and EGM2008 [units:  $\text{m}^2\text{s}^{-2}$ ]

Nodes	Resolution	Max.	Min.	Average	STD
518402	0.250 deg	43.423	-75.67	-0.8570	2.632
1440002	0.150 deg	23.798	-28.587	-0.1027	0.945
5760002	0.075 deg	7.632	-10.983	-0.0200	0.221
12960002	0.050 deg	2.378	-2.640	0.0002	0.065

software has been used. In case of FVM, a parallelization of algorithms using the MPI subroutines has been implemented. Table 2 shows statistical characteristics of the residuals between the FVM solutions and EGM2008 for different levels of the discretization (Fig. 5). Fig. 4b depicts the residuals for the finest discretization, i.e., the regular grid  $5 \times 5$  arc min on the ellipsoid and 400 m in radial direction ( $4320 \times 2160 \times 600$  finite volumes). In case of FEM, due to a limited access of the parallel version of the ANSYS software on the parallel cluster, only two solutions on coarser grids are presented (Table 3).

Graphs in Fig. 5 summarize all obtained statistical characteristics. They indicate convergence properties of all three methods in reconstructing the harmonic function given by EGM2008. The most detailed solutions by BEM and FVM show a very good agreement with EGM2008. The standard deviations are  $0.065$  and  $0.071 \text{ m}^2\text{s}^{-2}$  ( $\sim 7$  mm), the mean



**Computational Methods for High-Resolution Gravity Field Modeling, Fig. 3** 3D computational domain for global gravity field modeling by FEM or FVM

values are practically zero and the maximal and minimal residuals do not exceed  $\pm 2.7 \text{ m}^2\text{s}^{-2}$  ( $\sim \pm 27$  cm). Their plots in Fig. 4 show that the FVM solution includes some low-frequency error signal (Fig. 4b) whose amplitude is smaller than  $0.2 \text{ m}^2\text{s}^{-2}$  ( $\sim 2$  cm). The BEM solution shows a worse agreement in areas of high mountains, especially in Himalayas and Andes; however, it fits very well over oceans (Fig. 4a).

All three numerical methods can be also used for local gravity field modeling. The BEM approach has a drawback that it requires an integration over the whole boundary. In this case, local refinements of the triangulation can be done in order to reach detailed modeling in areas of interests. Figure 6 depicts such a local refinement in the area of New Zealand as well as the obtained local BEM solution (Čunderlík et al. 2010).

In case of FEM or FVM, the 3D computational domain can be restricted to the chosen region (Fig. 7). On the additional side boundaries, the Dirichlet BC can be prescribed similarly as they are prescribed on the upper boundary. Their values can be generated, e.g., from EGM2008. Figure 8 shows local modeling in the area of Slovakia using terrestrial gravimetric measurements and the FEM approach (Fašková et al. 2010). Figure 9 depicts local modeling in extremely mountainous regions of Himalayas and Tibet using the FVM approach (Macák et al. 2014).

## Summary

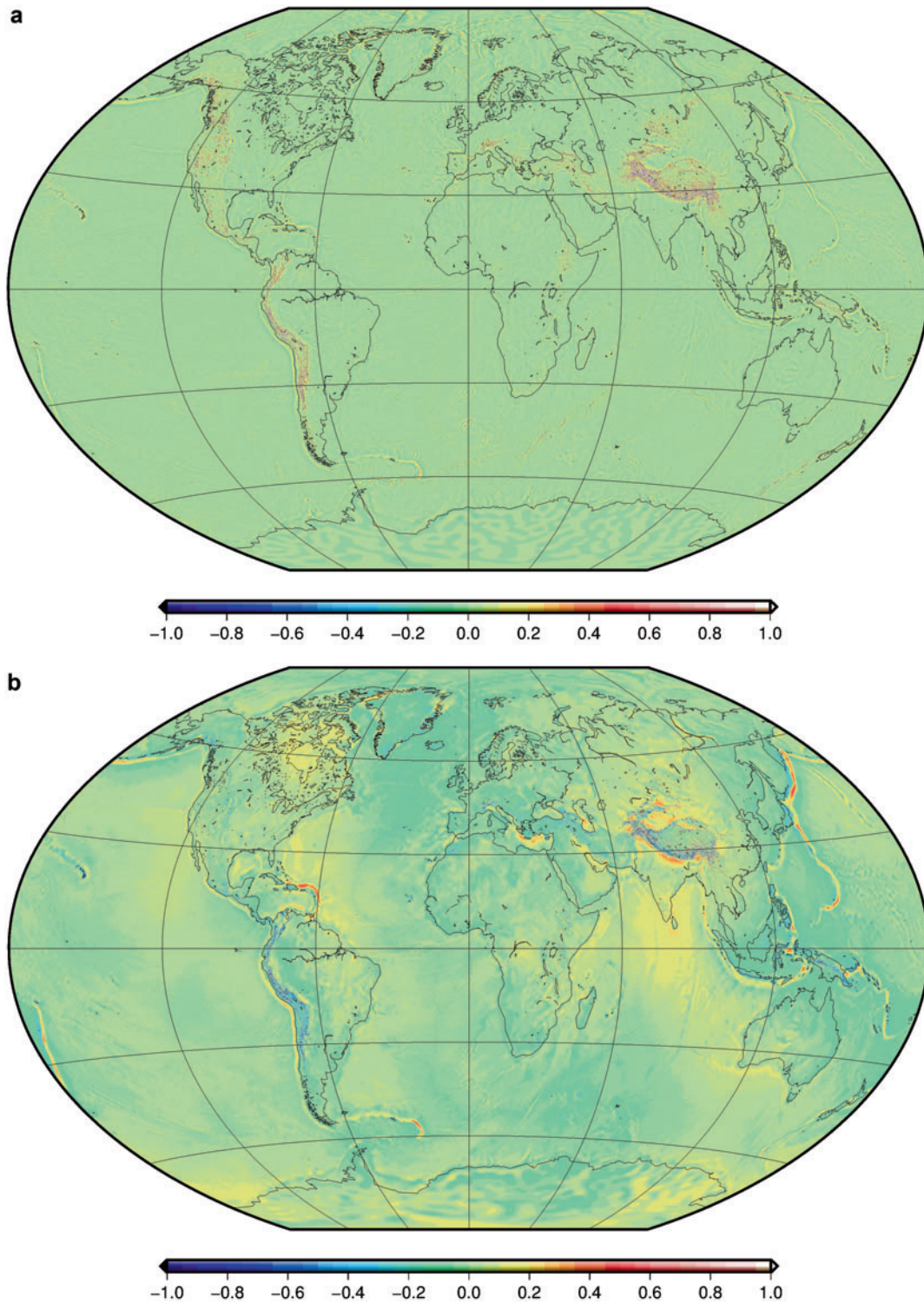
Computational methods like BEM, FEM, or FVM can be applied for high-resolution gravity field modeling. They are suitable to solve the geodetic BVPs in a space domain. In order to obtain precise numerical solutions, they require a detailed domain discretization. It naturally leads to large memory requirements and therefore large-scale computations need to be performed. Parallel implementations and high-performance computing on clusters with the distributed

**Computational Methods for High-Resolution Gravity Field Modeling, Table 2** Statistical characteristics of the residuals between the FVM solutions and EGM2008 [units:  $\text{m}^2\text{s}^{-2}$ ]

Nodes on ell.	Resolution	Max.	Min.	Average	STD
1036800	0.25000 deg	44.746	-68.946	-0.0262	1.552
2332800	0.16667 deg	6.684	-6.512	0.0000	0.178
9331200	0.08333 deg	2.648	-2.203	0.0000	0.071

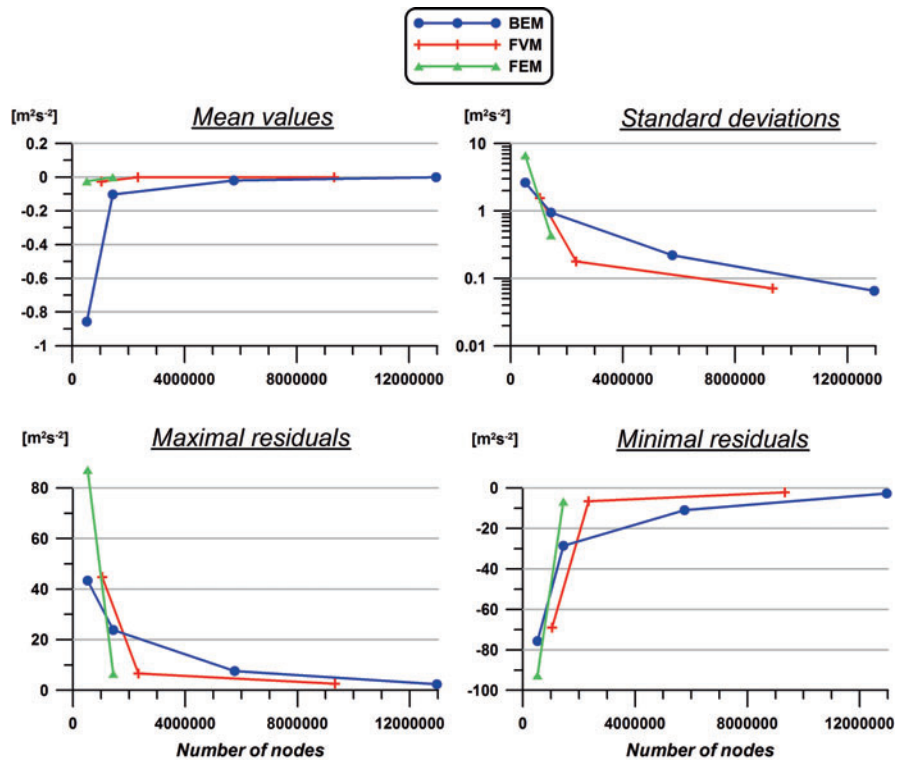
**Computational Methods for High-Resolution Gravity Field Modeling, Table 3** Statistical characteristics of the residuals between the FEM solutions and EGM2008 [units:  $\text{m}^2\text{s}^{-2}$ ]

Nodes on ell.	Resolution	Max.	Min.	Average	STD
518402	0.25 deg	87.088	-92.609	-0.0247	6.688
1440002	0.15 deg	6.602	-6.634	-0.0002	0.434

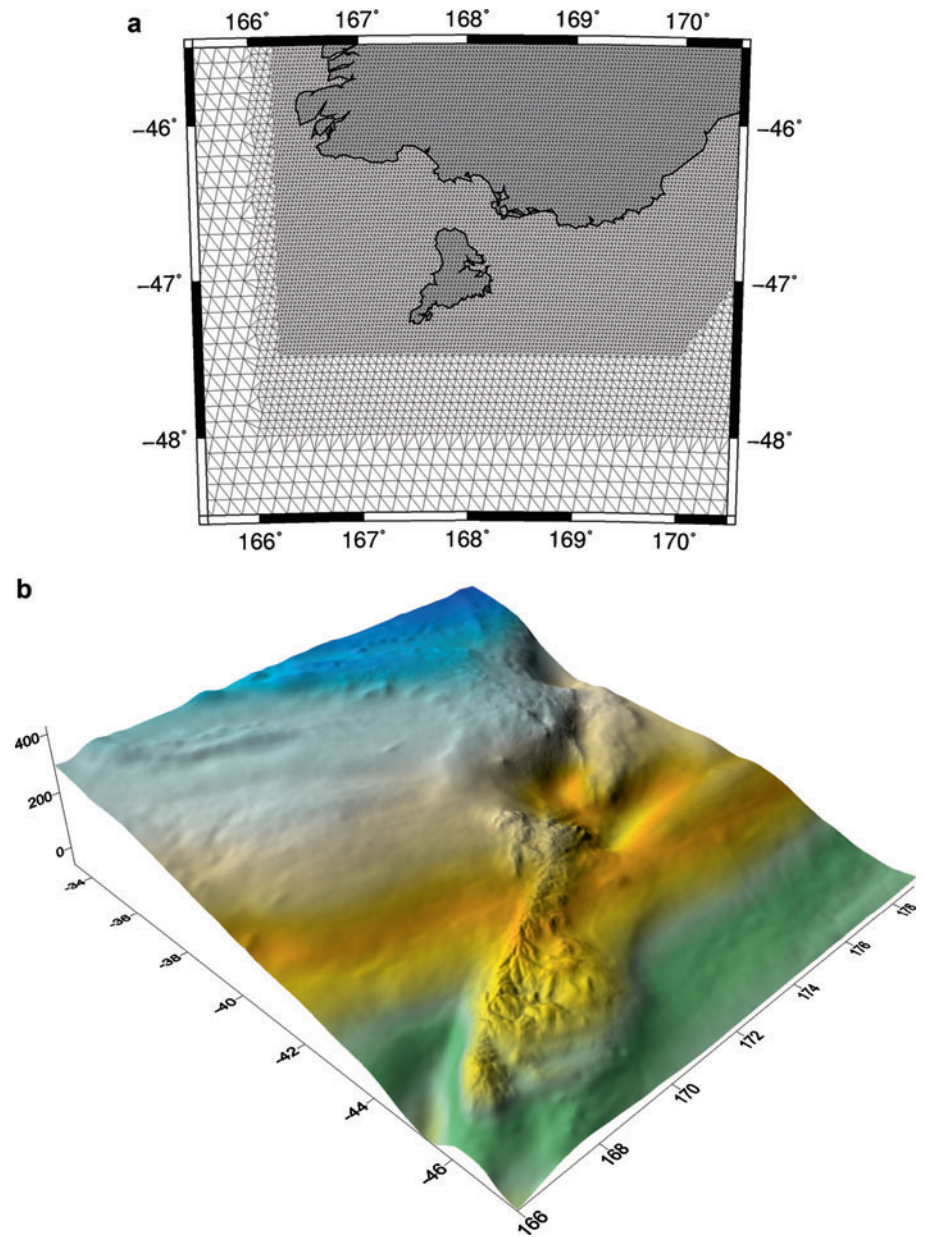


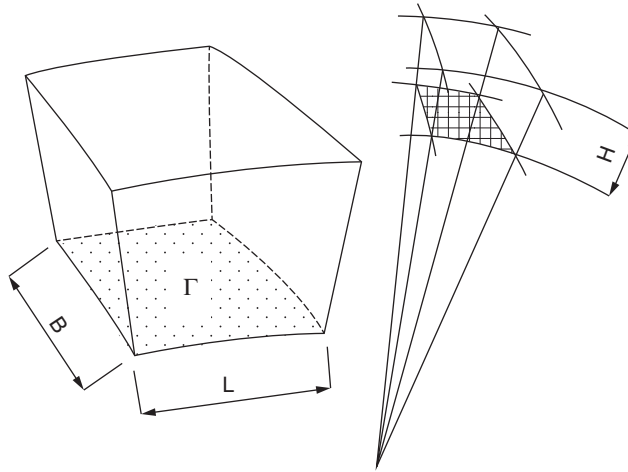
**Computational Methods for High-Resolution Gravity Field Modeling, Fig. 4** Residuals between (a) the BEM solution and EGM2008, and (b) the FVM solution and EGM2008 [units:  $\text{m}^2\text{s}^{-2}$ ]

**Computational Methods for High-Resolution Gravity Field Modeling, Fig. 5** Statistical characteristics of the residuals between the BEM, FEM, or FVM solutions and EGM2008



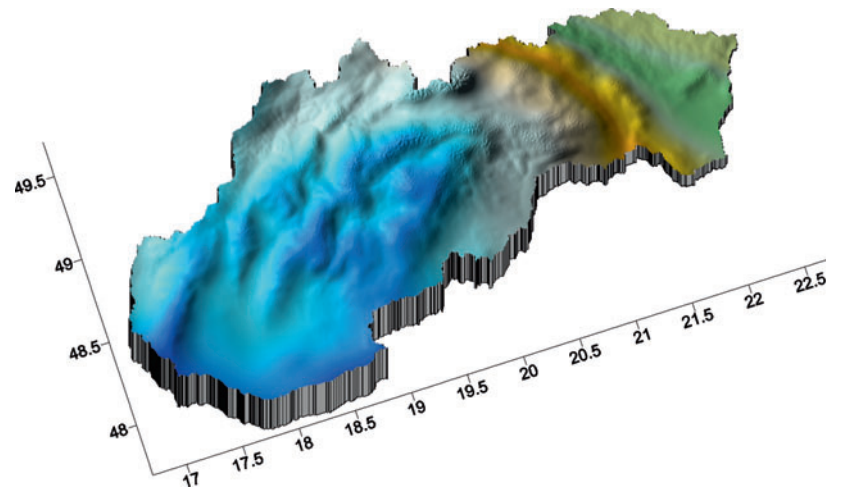
**Computational Methods for High-Resolution Gravity Field Modeling, Fig. 6** (a) Local refinement of the triangulation in New Zealand, and (b) the local BEM solution (source: Čunderlík et al. 2010)

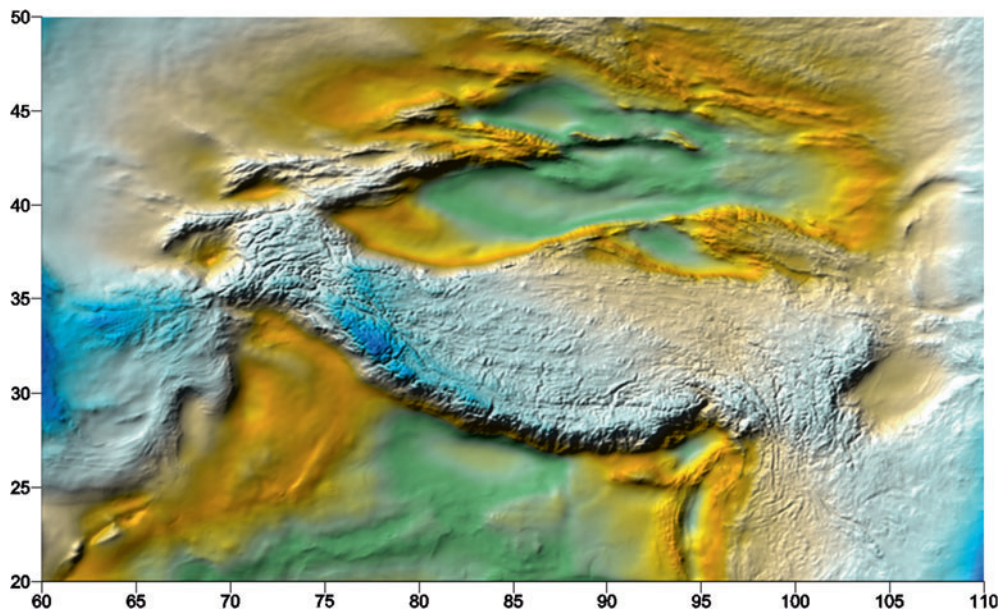




**Computational Methods for High-Resolution Gravity Field Modeling, Fig. 7** 3D computational domain for local gravity field modeling by FEM or FVM

**Computational Methods for High-Resolution Gravity Field Modeling, Fig. 8** Local gravity field modeling in Slovakia using the FEM approach





**Computational Methods for High-Resolution Gravity Field Modeling, Fig. 9** Local gravity field modeling in Himalayas and Tibet using the FVM approach

memory can overcome this problem. Then such computational methods can be efficiently used for global or local gravity field modeling representing alternative methods to classical approaches usually used in geodesy.

### Cross-References

- ▶ [\(Exact and Numerical Solutions of Geodetic Nonlinear Algebraic Equations\)?](#)
- ▶ [\(Oblique Derivative Problem and Multipole Methods\)?](#)
- ▶ [Boundary Value Problems in Physical Geodesy](#)
- ▶ [Geodetic Boundary Value Problem](#)
- ▶ [Global Models](#)
- ▶ [Regional Gravity Field Determination](#)
- ▶ [Spherical Harmonic Models](#)

### References

- Baláš, J., Sládek, J., Sládek, V., 1989. *Stress Analysis by Boundary Element Methods*. Elsevier, Amsterdam.
- Barrett, R., Berry, M., Chan, T.F., Demmel, J., Donato, J., Dongarra, J., Eijkhout, V., Pozo, R., Romine, C., Van der Vorst, H., 1994. *Templates for the Solution of Linear Systems: Building Blocks for Iterative Methods*, 2nd Edition. SIAM, Philadelphia, PA
- Brebbia, C.A., Telles, J.C.F., Wrobel, L.C., 1984. *Boundary Element Techniques, Theory and Applications in Engineering*. Springer-Verlag, New York.
- Brenner, S.C., Scott, L. R., 2002. *The Mathematical Theory of Finite Element Methods* 2nd ed. Springer-Verlag, New York.
- Čunderlík, R., Mikula, K., 2010. Direct BEM for high-resolution gravity field modelling. *Studia Geophysica et Geodaetica* 54(2): 219–238
- Čunderlík, R., Mikula, K., and Mojzeš, M., 2008. Numerical solution of the linearized fixed gravimetric boundary-value problem. *Journal of Geodesy* 82: 15–29
- Čunderlík, R., Tenzer R., Abdalla A., Mikula K., 2010. The quasigeoid modelling in New Zealand using the boundary element method. *Contributions to Geophysics and Geodesy* 40(4): 283–297
- Eymard, R., Gallouet, T., and Herbin, R., 2001. Finite volume approximation of elliptic problems and convergence of an approximate gradient. *Applied Numerical Mathematics* 37(1–2): 31–53
- Fašková, Z., Čunderlík, R. and Mikula, K., 2010. Finite Element Method for Solving Geodetic Boundary Value Problems. *Journal of Geodesy* 84: 135–144
- Hartmann, F., 1989. *Introduction to Boundary Elements. Theory and Applications*. Springer-Verlag, Berlin.
- Holota P., 1997. Coerciveness of the linear gravimetric boundary-value problem and a geometrical interpretation. *Journal of Geodesy* 71: 640–651.
- Koch, K.R., Pope, A.J., 1972. Uniqueness and existence for the geodetic boundary value problem using the known surface of the earth. *Bulletin Géodésique* 46: 467–476
- Laursen, M.E., Gellert, M., 1978. Some Criteria for Numerically Integrated Matrices and Quadrature Formulas for Triangles. *International Journal for Numerical Methods in Engineering* 12: 67–76
- Lucquin, B., Pironneau, O., 1998. *Introduction to Scientific Computing*. Wiley, Chichester.
- Macák, M., Minarechová, Z., Mikula, K., 2014. A novel scheme for solving the oblique derivative boundary-value problem. *Studia Geophysica et Geodaetica* 58(4): 556–570
- Mantič, V., 1993. A new formula for the C-matrix in the Somigliana identity. *Journal of Elasticity* 33(3): 191–201

- Minarechová Z., Macák M., Čunderlík R., Mikula K. 2015. High-Resolution Global Gravity Field Modelling by the Finite Volume Method. *Studia Geophysica et Geodaetica* 59(1): 1–20
- Pavlis, N.K., Holmes, S.A., Kenyon, S.C., and Factor, J.K., 2012. The development of the Earth Gravitational Model 2008 (EGM2008). *Journal of Geophysical Research* 117: B04406 DOI:<https://doi.org/10.1029/2011JB008916>
- Rektorys, K., 1974. Variační metody v inženýrských problémech a v problémech matematické fyziky. STNL, Praha. (In Czech)
- Schatz, A.H., Thomée, V., Wendland, W.L., 1990. *Mathematical Theory of Finite and Boundary Element Methods*. Birkhauser Verlag, Basel/Boston/Berlin.
- Šprlák, M., Fašková, Z., and Mikula, K., 2011. On the application of the coupled finite-infinite element method to geodetic boundary-value problem. *Studia Geophysica et Geodaetica* 55(3): 479–487